

# The Mechanical Behavior of Blends of Polyethylene, Polypropylene, and an Ethylene–Propylene Block Copolymer at $-20^{\circ}\text{C}$

VICKI FLARIS\* and ZBIGNIEW H. STACHURSKI

Mechanical Engineering Department, University of Melbourne, Parkville, Vic. 3052, Australia; Materials Engineering Department, Monash University, Clayton, Vic. 3168, Australia

## SYNOPSIS

Compatibilization is necessary for most binary blends which display poor mechanical properties. The addition of an ethylene–propylene block copolymer to a blend of isotactic polypropylene and linear low-density polyethylene alleviates the problem of poor adhesion at the interface. This was observed through the improvement in overall performance of the blend. It was noted that it is not solely the “interfacial agent” which is responsible for the improvement in impact strength of this blend. © 1992 John Wiley & Sons, Inc.

## INTRODUCTION

In this work attention has been focussed on the improvement of polypropylene's poor impact strength at low temperatures by blending with polyethylene.<sup>1–3</sup> The differences in the impact behavior of these two polymers relate to their glass transition temperatures. Polyethylene has a glass transition temperature at ca.  $-110^{\circ}\text{C}$ , as compared to polypropylene's lower glass transition temperature at about  $-22^{\circ}\text{C}$ .

In general, the mechanical properties of the binary blends are unsatisfactory as these two components are immiscible and incompatible. This paper presents a study on the compatibility of these blends with the addition of a ternary component. The compatibilizer chosen was an ethylene–propylene block copolymer as it is expected thermodynamically to sit at the interface between the two components. The ethylene–propylene segments are incompatible with each other on the molecular scale but each segment is compatible with one of the phases.<sup>4–7</sup>

## EXPERIMENTAL

### Materials and Blend Preparation

The starting materials used were: isotactic polypropylene (i-PP) ( $\rho = 0.905 \text{ g/cm}^3$ ), linear low-density polyethylene (LLDPE) ( $\rho = 0.919 \text{ g/cm}^3$ ), and ethylene–propylene block copolymer (EP) ( $\rho = 0.902 \text{ g/cm}^3$ ). The tradename of the EP copolymer is GXM104. They were used as standard commercial grade materials with typical additives present.

The blends were prepared by tumble blending for 15 min (the proportions are stated in Table I) and then melt-blending in a 1.5 in. Johns single-screw extruder using temperature profile 190, 200, 210, 220, 230, and  $230^{\circ}\text{C}$ , for zones 1–4, the head and the die zone, respectively. Then followed the quenching in water of the laces, their blow drying, and finally their granulation. The unblended materials were passed through an identical process of extrusion so as to give them the same history as the blend samples.

### Polymer Characterization

The materials were characterized using dynamic mechanical thermal analysis (DMTA), differential scanning calorimetry (DSC), and gel permeation

\* To whom correspondence should be addressed.

**Table I Blend Compositions<sup>a</sup>**

Blend	% Composition		
	PP	LLDPE	EP
1	100	0	0
2	80	20	0
3	79.2	19.8	1
4	72	18	10
5	0	100	0
6	98.8	0	1.2 <sup>b</sup>
7	88	0	12 <sup>b</sup>
8	0	0	100 <sup>b</sup>

<sup>a</sup> There is minimal error associated with the composition because these samples were produced in large quantities. The blend compositions were checked after mixing using a differential scanning calorimeter (DSC).

<sup>b</sup> These samples were prepared as reference materials with respect to the PP/EP/LLDPE blends.

chromatography (GPC) to determine the glass transition temperature, melting temperature, and molecular weight distribution respectively. These results are summarized in Table II.

The measurements on the Polymer Laboratories DMTA were made in the temperature range of  $-120$ – $50^\circ\text{C}$  on samples of the following dimensions: length 20 mm, width 10 mm, and thickness 1 mm. They were run in a single-cantilever mode at frequencies of 0.3, 3.0, and 30 Hz. Flat specimens of about 10 mg weight, encapsulated in aluminium pans, were used for DSC measurements on a Mettler DSC 20. The samples were heated from 50 to  $250^\circ\text{C}$  at a programmed heating rate of  $10\text{ K min}^{-1}$ . All measurements were made under a nitrogen atmosphere (flow rate  $50\text{ mL/min}$ ). GPC samples were run on a Waters 150C GPC combined with a Viscotek differential viscometer at  $140^\circ\text{C}$ , using 1,2,4-trichlorobenzene as the solvent. Absolute molecular weights were calculated using the principle of universal calibration.

The microstructure of these blends was studied using the technique of scanning electron microscopy (SEM). Fractured Charpy impact samples were etched for 15 min at  $70^\circ\text{C}$  in an acid mixture composed of 19.8% hydrochloric acid, 61% phosphoric acid, 2.7% chromium trioxide, and 16.5% water. This etched out the block copolymer but had no effect on LLDPE or PP. The samples were then water cooled on a cold stage prior to gold coating to a thickness of 32 nm in an argon atmosphere. The microscopes used were an ISI Mini SEM and a Phillips SEM 515 model.

## Mechanical Testing

Samples for tensile tests and Charpy impact tests were injection-molded from the blends. The tensile samples were molded using a Battenfeld injection molder at  $245^\circ\text{C}$  into dumbbell shapes of 3.0 mm thickness, 12.6 mm width, and with a gauge length of 50 mm. All samples were annealed at  $95^\circ\text{C}$  for 2 h and slowly cooled in order to alleviate the problems of orientation and internal stressing. The tests were carried out using an Instron Model 1026 tensile testing machine at a crosshead speed of 1 mm/min. For measurement of Young's modulus an appropriate extensometer was used. The samples for the Charpy impact test were also injection molded at  $245^\circ\text{C}$  into  $6 \times 13 \times 130$  mm thick bars and were then machined down to  $6 \times 5 \times 45$  mm. A single point cutter was used to centrally notch each specimen with a  $45^\circ$  V-notch. Sixteen samples were tested at four notch depths. The notch depths varied between 30 and 60%. The samples were in an ethanol/dry ice mixture for 0.5 h to achieve temperature equilibrium and then tested using a Hounsfield impact tester. It is well known that ethanol does not affect the properties of polypropylene or polyethylene. The tests were carried out at  $-20^\circ\text{C}$  as these blends were prepared with the primary aim of improving PP's impact strength at low temperatures.

## RESULTS AND DISCUSSION

### Morphology of Blends

Scanning electron microscopy revealed the location of the components in the blends. Typical morphology of the fracture surfaces is shown in Figure 1. The compatibilizer forms shells around the LLDPE

**Table II Polymer Characterization**

Material	$T_g^a$ ( $\pm 0.5^\circ\text{C}$ )	$T_m^b$ ( $\pm 0.5^\circ\text{C}$ )	$\bar{M}_n$	$\bar{M}_w/n^c$
PP	$-22(+3)^d$	166.4	57000	5.14
LLDPE	-110	122.5	30300	3.70
EP	-49	166.8	52400	5.65

<sup>a</sup>  $T_g$  values were measured using a Polymer Labs DMTA in the temperature range of  $-120$ – $50^\circ\text{C}$  at a heating rate of  $2^\circ\text{C/min}$ .

<sup>b</sup>  $T_m$  values were measured using a Mettler DSC at a heating rate of  $10^\circ\text{C/min}$ .

<sup>c</sup> MW measured using ICI GPC.

<sup>d</sup> PP has apparently two glass transitions.

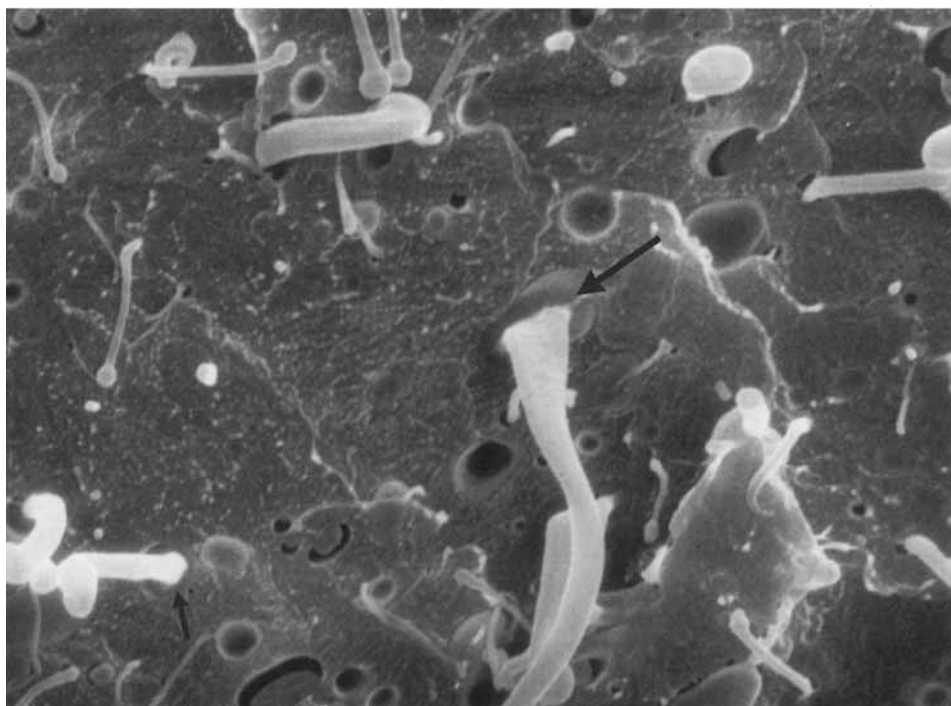


**Figure 1** Morphology of impact surface of blend 4, fractured at  $-20^{\circ}\text{C}$  (SEM  $\times 4500$ ).

particles as well as itself, forming separate particles dispersed in the matrix. The shell morphology of the EP copolymer has been reported for the PP/EP/HDPE ternary blend previously.<sup>8</sup> The formation of the shell around the LLDPE was observed in both the ternary blends containing 1% EP and 10% EP. However, in the blend containing 1% EP, crescent shaped gaps around the LLDPE occlusions were also observed suggesting incomplete and insufficient coverage by the block copolymer around the LLDPE particles.

The sizes of LLDPE inclusions vary from 0.9 to 1.3  $\mu\text{m}$  in diameter in the binary blends. In the etched ternary blends there are crescent-shaped holes observed between LLDPE and PP as well as circular holes left in the material. The circular holes after etching are 1.2–1.6  $\mu\text{m}$  in diameter. This indicates that LLDPE alone cannot have occupied this space and that the holes must have contained block copolymer. Charpy samples were also fractured in liquid nitrogen to further confirm the arrangement of the components. It would seem from Figure 2 that there are a few LLDPE occlusions embedded in the block copolymer.

DMTA results provide further evidence about the immiscibility of the blends as separate glass transitions were observed for each component. With PP there are apparently two glass transitions.<sup>9</sup> It is

composed of amorphous phase A and amorphous phase B, which have transitions at  $-22$  and  $+3^{\circ}\text{C}$ , respectively. The glass transition of LLDPE was measured at about  $-110^{\circ}\text{C}$  and its  $\beta$  transition at  $-35^{\circ}\text{C}$ . We observed in blend 4 that the  $\beta$  transition of polyethylene has shifted by about  $10^{\circ}\text{C}$  to lower temperatures. This shift may be related to the fact that the ethylene segment of the block copolymer becomes partially miscible with the PE component.

#### Young's Modulus of Blends

As a starting point, it can be assumed that our heterogeneous materials may be described adequately as consisting of a homogeneous and isotropic matrix, in which particles of a second homogeneous phase are dispersed. Assuming that the volume concentration of the particles is uniform, it should be possible in principle to calculate the properties of multiphase materials in terms of the properties of its constituents. The mechanical results are summarized in Table III and Figures 3–6.

As a first approach we may consider the simple law of mixtures for the Young's modulus of the blends. The equation for the upper bound of the modulus is given by<sup>10</sup>

$$E_b = E_1\phi_1 + E_2\phi_2 \quad (1)$$

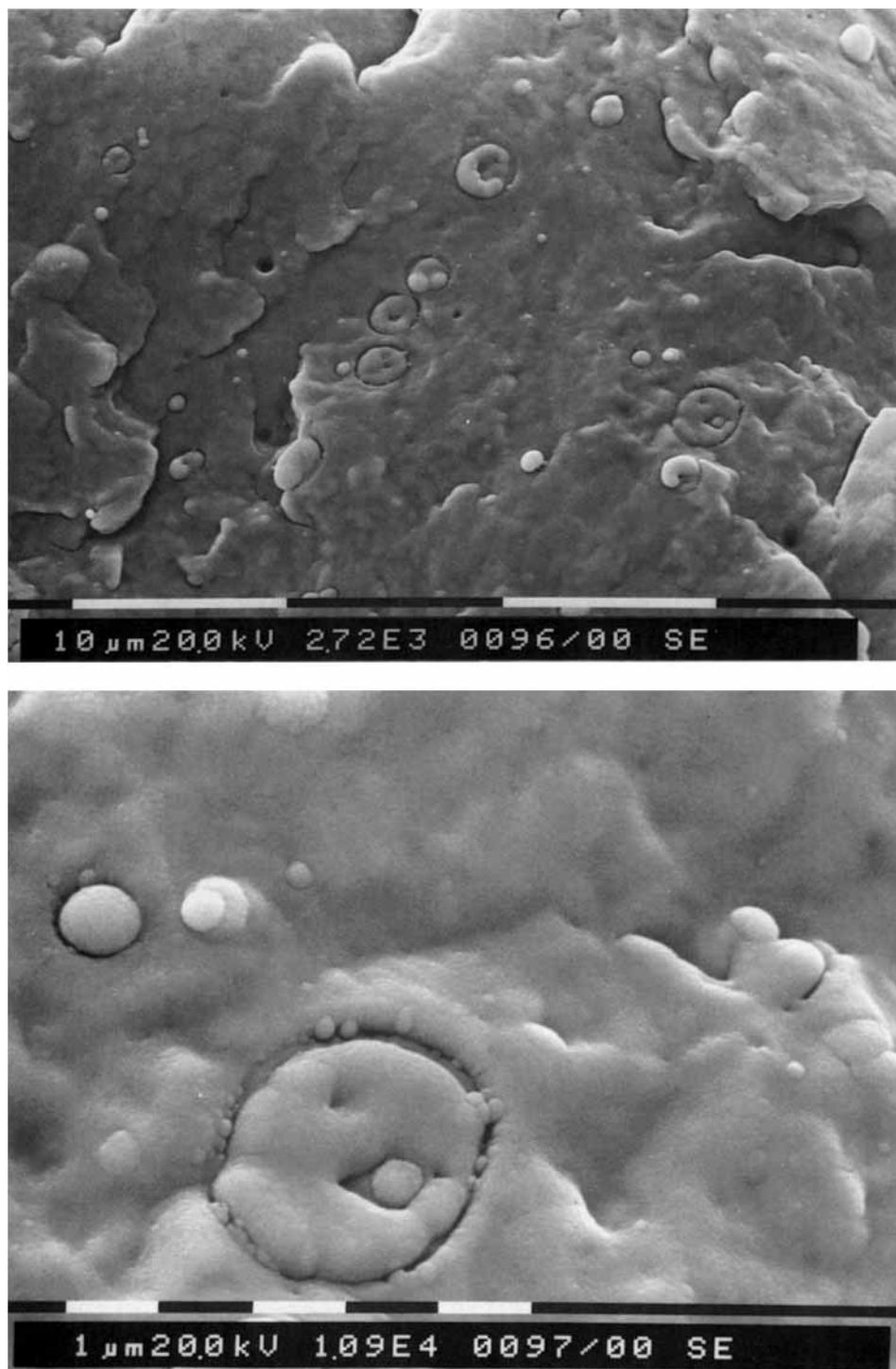


**Figure 2** SEM micrographs of impact surfaces of blend 4 fractured at liquid nitrogen temperature.

The corresponding equation for the lower bound is given by

$$\frac{1}{E_b} = \frac{\phi_1}{E_1} + \frac{\phi_2}{E_2} \quad (2)$$

where  $E_1$  and  $E_2$  are the Young's moduli of PP and LLDPE, respectively, and  $\phi_1$  and  $\phi_2$  are the volume fractions of PP and LLDPE, respectively. Figure 3 shows plots of eqs. (1) and (2) fitted to our data from Table III, as well as the experimental modulus

**Table III Summary of Mechanical Results at  $-20^{\circ}\text{C}^a$** 

Blend	$E$ (GPa)	$\sigma_y$ (MPa)	$G_c$
1	4.5	57.3	0.82
2	3.5	52.2	1.21
3	3.4	44.4	1.45
4	3.4	42.3	2.06
5	0.7	13.9	16.0
6	4.2	54.2	0.55
7	4.8	51.4	1.08
8	2.5	35.2	3.77

<sup>a</sup> There is less than 5% error associated with the yield stress values and less than 10% error with the modulus and Charpy impact values.

data for the binary and ternary blends of PP and LLDPE. The experimental values for the Young's modulus lie between these two bounds with the exception of one point. In fact, the points are essentially at the upper bound, indicating that a simple additive law of mixtures can be used as a first approximation. More detailed study and analysis may reveal special relationships and microstructures, particularly at the high PE content side of the composition range.

A different approach was taken by Kleiner et al.<sup>11</sup> who proposed an empirical equation of second order that can describe a synergistic effect of blending on modulus in terms of an interaction parameter  $\beta$ :

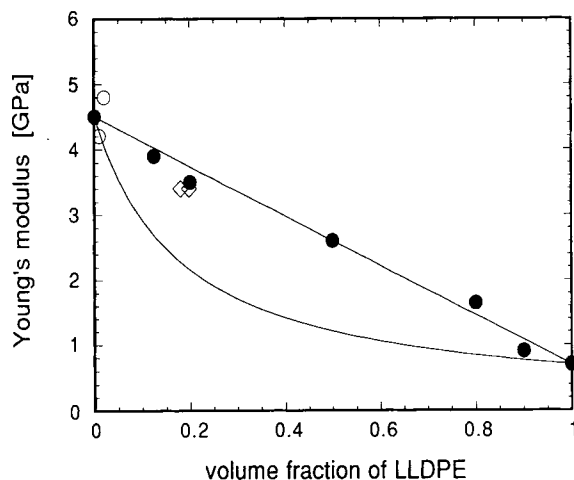


**Figure 3** Young's modulus versus volume fraction of LLDPE data at  $-20^{\circ}\text{C}$ . Crosshead speed 1 mm/min: (○) data for ternary blends 6 and 7; (◇) data for ternary blends 3 and 4 from Table III; (●) binary blends 1, 2, and 5 from Table III as well as unlisted data.

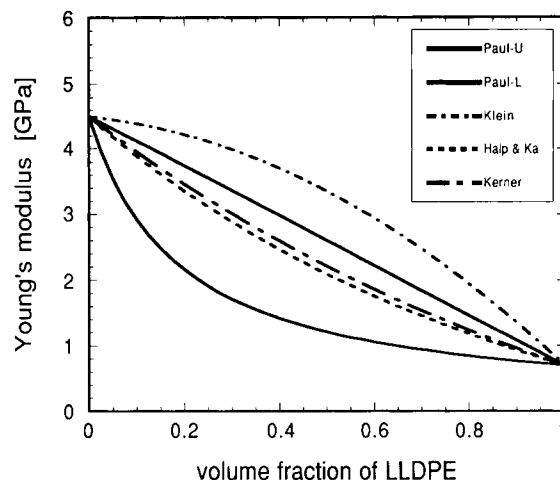


**Figure 4** Variation of Young's modulus with composition for two phase composite and blend materials according to eqs. (1)–(5).

$$E_b = E_1\phi_1 + E_2\phi_2 + \beta\phi_1\phi_2 \quad (3)$$

For our data a reasonably good fit can be obtained as  $\beta$  approaches zero. The relationship is thus reduced to the equation derived by Paul describing the upper bound for the elastic modulus in tension for a two-phase blend. By contrast, Kleiner and his co-workers obtained a value of  $\beta = 2$  for blends of polystyrene with polyphenylene oxide of low molecular weight ( $M_w \approx 10^4$ ). They have shown that a good correlation exists between the modulus of elasticity and the density as a function of blend composition.

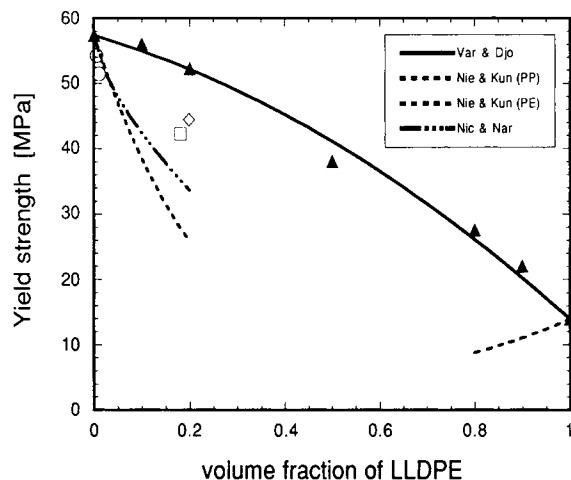


**Figure 5** Dependence of yield strength on composition. Experimental data obtained at  $-20^{\circ}\text{C}$  and crosshead speed of 1 mm/min: (▲) binary blends; (○) blends 6 and 7; (◇, □) blends 3 and 4 from Table III. Continuous and broken lines represent equations (7), (9) and (10).

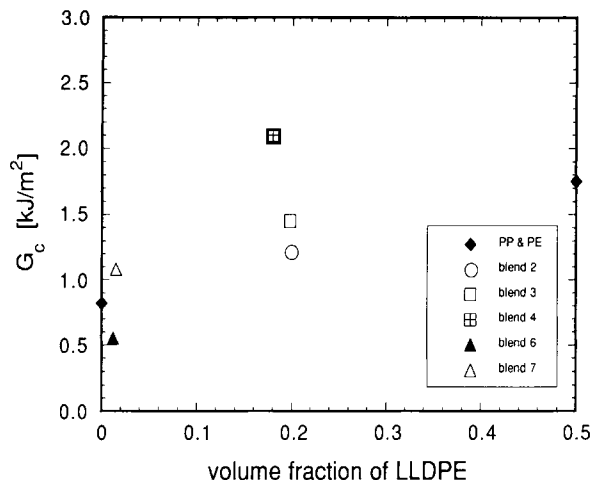


**Figure 6** Variation of strain energy release rate with volume fraction of LLDPE, obtained from Charpy impact tests carried out at  $-20^{\circ}\text{C}$ , for the binary and ternary blends.

If we consider the blends not as a continuum of two phases, but rather as a matrix with inclusions, then the theories of Kerner<sup>12</sup> and Halpin and Kardos<sup>13</sup> become relevant. In this approach, the dependence of modulus on the volume fraction of inclusions is described by the Kerner equation as follows:

$$E_b = E_1 \frac{\phi_2(\alpha E_2 - \beta) + \beta}{\phi_2(\alpha E_1 - \beta) + \beta} \quad (4)$$

where  $\alpha = [(7 - 5\nu_1)E_1 + (8 - 10\nu_1)E_2]^{-1}$  and  $\beta = [15(1 - \nu_1)]^{-1}$ , with  $\nu$  being Poisson's ratio. The equation is universal in the sense that the volume fraction of inclusions can vary from zero to 100%, and correspondingly the matrix can be either PP or LLDPE. It turns out that the above equation is not very sensitive to the value of Poisson's ratio between 0.2 and 0.5, so much so that Dumoulin et al.<sup>14</sup> used different values (for polyethylene-rich blends,  $\nu_{\text{PE}} = 0.48$  and  $\nu_{\text{PP}} = 0.43$ , and for polypropylene-rich blends,  $\nu_{\text{PE}} = 0.48$  and  $\nu_{\text{PP}} = 0.8$ ) to fit their data to the equation. There is no justification for the unrealistic value of  $\nu_{\text{PP}} = 0.8$ . If the volume of material remains unchanged, then  $\nu = 0.5$  and  $\nu < 0.5$  for materials which display an increase in volume.<sup>15</sup> Dumoulin et al. used the constants  $\nu_1$  and  $\nu_2$  as empirical factors rather than the Poisson's ratio in order to fit the equation.

The theory of Halpin and Kardos is based on Kerner's and Hill's<sup>16</sup> approach. They have derived an equation for the modulus of a composite material

consisting of a matrix and inclusions, which can be written as follows:

$$E_b = E_1 \frac{1 - AB\phi_2}{1 + B\phi_2}, \quad B = \frac{E_1 - E_2}{AE_1 + E_2} \quad (5)$$

The constant  $A$  depends on the stress distribution in the composite, and for spherical particles has a value of 2.

Yet another approach was taken by Smallwood,<sup>17,18</sup> who derived the following equation for a system with perfect adhesion between the matrix and particles:

$$E_b = E_1(1 + 2.5\phi_2 + 14.2\phi_2^2) \quad (6)$$

We note that the above equation was derived for the stiffening effect in rubber due to spherical filler particles. In our case the equation could be at best applied to the blends in which PE is the matrix of low modulus and PP is in the form of rigid particles. Another equation was developed by Sato and Furukawa<sup>19</sup> to describe a system of hard particles in plastics, where the adhesion between the two phases is weak. Both Smallwood and Sato and Furukawa equations apply over limited ranges of volume fractions, and can be approximated by the general equation (5).

Figure 4 shows plots of eqs. (3)–(5). Note that Kerner's and Halpin and Kardos equations are indistinguishable if the experimental error limits associated with our results are taken into account. Klein's, and, to some extent, Smallwood's equations are the only ones capable of showing a synergistic effects leading to modulus values above the upper bound. From a comparison of Figures 3 and 4 it becomes clear that our results for the binary blends are represented best over the whole range of volume fractions by the simple law of mixtures [eq. (1)]. Paul used energy theorems of elasticity to derive this equation. An implicit assumption in this derivation is that of the continuity of stress in the two phases (matrix and inclusion), and, as a consequence, the discontinuity of strains, since the elastic moduli of the two phases are very different. This condition would be satisfied if there was no adhesion between the two polymers. It would also be satisfied if the interface is amorphous and rubbery, and hence easily conforming to the requirement of discontinuity of strain. Such an interface should consist of a layer of about 1–2 nm in thickness, made up of a mechanical mixture of PP and LLDPE chains, which are in a noncrystalline state.

Finally we make the point that the modulus of

the ternary blends does not differ to any significant extent from that of the binary blends, considering the few data points that we have and noting that the data for the ternary blends are superimposed onto a binary blend diagram. This appears to be surprising at first since the modulus of EP is essentially halfway between those of PP and LLDPE whereas the discussion above called for a rubbery interface. We believe that the solution is in the understanding that the EP is not necessarily the interface, but rather that the blend consists of three phases with two soft interfaces between each, that is, at the PP/EP boundary and the EP/LLDPE boundary.

As a final comment, it is interesting to note that for the PC/PE and PC/PS blends<sup>18</sup> the variation of modulus with volume fraction showed a substantial dip below the straight line of the upper bound. Kunori and Geil<sup>18</sup> explained these in terms of (i) anisotropic domains and (ii) foam or loose particle approximation. In our opinion the latter approximation is not substantiated enough. We accept that there may not be any adhesion between the PE/PC phases as is shown by the micrographs of the fractured surfaces. However, the optical micrographs of the unfractured specimens do not show any looseness, and since the Poisson's ratio of the two polymers is approximately the same, then, under tensile deformation, the particles must contribute to the resistance to deformation of the blend, and consequently to the Young's modulus of the blend.

### Yield Strength of Blends

The yield strength is defined here as the first point of maximum stress on a stress-strain curve. When the data from Table III are plotted against volume fraction, as shown in Figure 5, then to a first approximation the experimental results follow a linear relationship.

There are few theories describing the yield strength of polymer blends in terms of composition. One such "rule of mixtures" for yield strength, proposed by Varin and Djokovic,<sup>20</sup> is as follows:

$$\sigma_b = \sigma_1\phi_2 + \sigma_2\phi_2 + \gamma\phi_1\phi_2 \quad (7)$$

where  $\sigma_b$  is the tensile yield strength of the blend,  $\sigma_2$  is the yield strength of the inclusion,  $\sigma_1$  is the yield strength of the matrix,  $\gamma$  is the interaction term, in this case between polypropylene and polyethylene, and  $\phi$  has the usual meaning of volume fraction. We fit eq. (7) to the experimental results and found  $\gamma$  to vary between +22 to +42 across the

full composition range. This indicates that the interaction between the two phases is not constant but depends on the relative fractions of the two components. The curve in Figure 5 is for  $\gamma = 22$ .

Neilsen<sup>21</sup> and Leidner et al.<sup>22-24</sup> proposed that the tensile strength of composite materials, consisting of a matrix with spherical inclusions, can be related to the area fraction of the dispersed phase, with a general equation of this form:

$$\sigma_b = K\sigma_1(1 - \phi_2^n) \quad (8)$$

The parameter  $K$  reflects the possible modification in the strength of the matrix due to the presence of the second phase, but normally  $K = 1$  if the two are immiscible. Leidner concluded that if there is no cohesion between the inclusions and the matrix, then the yield strength of the blend should be decreasing as the volume fraction to the first power, in which case  $n = 1$  in eq. (8). However, further considerations by Nicolais and Narkis<sup>25</sup> resulted in a modified equation:

$$\sigma_b = \sigma_1(1 - 1.21\phi_2^{2/3}) \quad (9)$$

The value of the constant in front of  $\phi_2$  is chosen so that  $\sigma_b = 0$  when  $\phi = 0.75$  (maximum packing by filler). Another approach was taken by Neilsen<sup>26</sup> and Kunori and Geil,<sup>27</sup> who suggested that in a blend, where the two components display considerable decohesion, the particles do not contribute to strength and can be thought of as voids. In this case the following equation should describe the tensile strength:

$$\sigma_b = \sigma_1 \exp(-\alpha\phi_2) \quad (10)$$

where  $\alpha$  is an empirical constant. However, Schragger<sup>28</sup> included microstructural features in the analysis of stress distribution, and proposed the following definite physical meaning for  $\alpha$ :

$$\alpha = \frac{V_\alpha + V_i}{V_i} \quad (11)$$

where  $V_\alpha$  is the volume of the matrix surrounding an embedded particle and affected by its presence, as is defined by eq. (12) below.  $V_i$  is the volume of the dispersed particle and is described by eq. (13).

$$V_\alpha = 4\pi[(R + \Delta r)^3 - R^3]/3 \quad (12)$$

$$V_i = 4\pi R^3/3 \quad (13)$$

Fitting our data to eq. (10) results in  $\alpha = 0.7\text{--}0.9$  for the PP-rich blends. This is meaningless since by definition  $\alpha > 1$ . However, using eqs. (12) and (13) instead to determine  $\alpha$  from the observed microstructure, we get a value between 3.2 and 4.4 (assuming that the affected area around the inclusions is somewhere between  $0.3R$  and  $0.5R$ ). These values were used in eq. (10) shown by the broken lines in Figure 5.

Equations (8)–(10) were developed to describe the reduction in strength due to inclusions whereas we find that the yield strength data can be best fit, to a first approximation, by a line slightly curving upwards. This is summarized in Figure 5, which shows experimental data and plots of eqs. (7), (9), and (10).

The dependence of yield stress on volume fraction was examined making the assumption that similar type of dependence exists as the dependence of the tensile strength on volume fraction. From Figure 5 it can be seen that all the experimental values lie close to the line plotted from eq. (7), suggesting the existence of an intermixed zone and some interfacial adhesion between the two phases. Greco<sup>29</sup> and his co-workers have measured yield strength in the same way on similar blends. They reported that at the lower volume fractions of PE the yield stress of the blends lies well above the solid line. This they related to the marked reinforcing effect of the PE component on PP. Apparently the PE inclusions delay the neck formation, and so the yield stress obtained for the blends is higher than the additive value of the pure components. We did not, however, observe this in our binary blends.

The experimental yield strength values for the ternary blends dropped by approximately 20% in relation to the binary blends. One conclusion is that the EP block copolymer, which has double the yield strength of LLDPE, is not as effective as LLDPE in delaying neck formation in the blend sample.

### Toughness of Blends

The value of  $G_c$ , the critical strain energy release rate at fracture, was used to assess the impact behavior of our blends.  $G_c$  can be obtained directly from absorbed fracture energy measurements under the condition that the deformation is elastic. Marshall et al.<sup>30</sup> and Brown<sup>31</sup> have independently shown that the fracture mechanics approach can be applied to impact testing if this assumption is satisfied. We have carried out our measurement at  $-20^\circ\text{C}$ , and observed very little nonelastic deformation of the specimens.

The values of the critical strain energy release rate were taken as the gradients from the plots of the fracture energy  $U_f$ , against the factor  $\Phi BW$  for each blend.  $\Phi$  is the geometry factor and is calculated for measured crack lengths using tables of values for standard Charpy specimens, derived from numerical stress analysis.<sup>32</sup>  $B$  and  $W$  are the thickness and width of the specimen respectively. The Charpy impact results are summarized in Figure 6. From the graph it can be seen that with the addition of 20% LLDPE the impact strength of PP improves by roughly 50%. This improvement in impact strength however is not significant as has been reported by Teh<sup>33</sup> and others.<sup>2</sup>

The addition of 1% EP block copolymer to the 20% LLDPE binary blend improves its impact strength by a further 20%. With the ternary blend containing 10% EP block copolymer at  $-20^\circ\text{C}$ , a 150% increase in the impact strength of PP is obtained, which corresponds to a 50% increase in the impact strength of the binary blend containing 20% LLDPE.

There were two reasons for preparing ternary blends using 1% and 10% EP block copolymer. One was to establish the amounts required to fully compatibilize our system and the second to determine whether the improvements in impact strength were related to the fact that the EP block copolymer was acting as a good interfacial agent. We prepared as reference samples, binary blends of PP and EP close to the proportions present in the ternary blend (compare blends 3 and 4 with blends 6 and 7). We note that in blend 6 the impact strength is less than of blend 3 and of pure PP, suggesting a negative effect of EP alone on the PP matrix. It is therefore evident that the EP block copolymer in blend 3 is playing a crucial role as an interfacial bonding agent. A comparison of blends 4 and 7 suggests that roughly

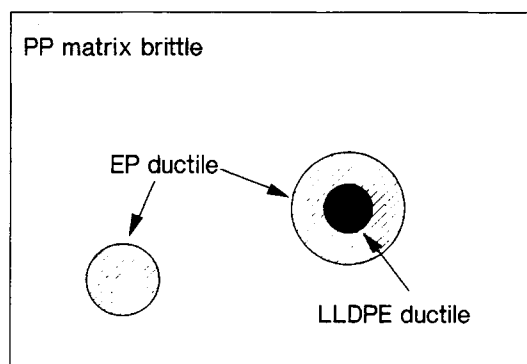


**Figure 7** Proposed model of the microstructure of a PP/EP/LLDPE ternary blend.



50% of the improvement in impact strength is due to the EP block copolymer acting as a compatibilizer.

### Toughening Model

We hypothesize that there are two mechanisms of toughening.<sup>34</sup> If we consider Figure 7, as an idealized microstructure of the ternary blend, then the first mechanism we propose is that of energy absorption by the drawing of the polyethylene occlusion [see Fig. 8(a)]. The corresponding microstructural features of the drawn polyethylene are shown in Figure 1. The second mechanism is related to the matrix being toughened through the introduction of the soft particle. It is well known that the addition of rubber particles to glassy polymers increases their toughness. We propose that the second mechanism of toughening of our blends is of similar nature. We would expect these inclusions to act as stress concentrators and so to initiate crazing and plastic deformation in the matrix. Then it follows that the impact resistance of the homopolymer (*i*-PP) can be increased as plastic deformation and orientation of the ethylene-propylene copolymer absorbs in part the mechanical energy of the impact.<sup>35,36</sup>

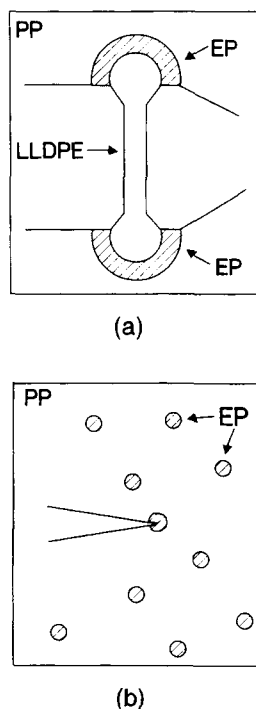


**Figure 8** Mechanisms of energy absorption in the ternary blend: (a) by drawing of the ductile phase (LLDPE); (b) by reduction of stress concentration at the tip of the crack by the presence of soft particles.

### CONCLUSION

The addition of LLDPE alone is ineffective in improving the impact strength of PP to acceptable levels for applications at low temperatures. This may be due to the fact that the dispersed LLDPE particles are present as a minor percentage and therefore cannot initiate plastic deformation, crazes, nor arrest crack growth to the extent of the EP copolymer. It may also be related to the poor adhesion between LLDPE and PP at the interface. From our results there is a strong suggestion that adhesion between these two components is improved by the presence of the ethylene-propylene block copolymer as each segment anchors firmly in the phase it is trying to compatibilize. The improvement noted in impact strength at the 10% level of EP is not due entirely to interfacial activity. This implies that to maximize the impact strength of a blend one must consider a ternary component which will not only improve the adhesion of the two components but will also reinforce the matrix.

The authors would like to thank ICI Australia Operations Pty. Ltd. for the supply of the materials and for the use of their extruding, injection-molding, and GPC facilities. We would also like to thank Telecom Australia and Amcor Ltd. for the use of their DMTA. The initial part of the research program was supervised by Mr. Oscar Delatycki and Vicki Flaris is indebted to him for his help. V. F. would also like to thank Dr. Doug Borland for helpful discussion and reading of the manuscript.

### REFERENCES

1. J. Kolarik, G. L. Agrawal, Z. Krulis, and J. Kovar, *Polym. Compos.*, **7**(6), 463 (1986).
2. J. Kolarik, J. Velek, G. L. Agrawal, and I. Fortelny, *Polym. Compos.*, **7**(6), 472 (1986).
3. D. Yang et al., *Polym. Eng. Sci.*, **24**(8), 612 (1984).
4. M. J. Folker and A. Keller, in *Block and Graft Copolymers*, J. J. Burke and V. Weise, Eds., Syracuse University Press, Syracuse, NY, 1973.
5. N. G. Gaylord, *Am. Chem. Soc. Adv. Chem. Ser.*, **142**, 76 (1975).
6. D. R. Paul, in *Polymer Blends*, D. R. Paul and S. Newman, Eds., Academic, New York, 1978.
7. G. Riess and Y. Jolivet, *Am. Chem. Soc. Adv. Chem. Ser.*, **142**, 243 (1975).
8. F. C. Stehling, T. Huff, and C. S. Speed, *J. Appl. Polym. Sci.*, **26**, 2693 (1981).
9. M. Jarrigeon, B. Chabert, D. Chatain, C. Lacabanne, and G. Nemoz, *J. Macromol. Sci. Phys.*, **B17**, 1 (1980).

10. B. Paul, *Trans. Metallurg. Soc. AIME*, **218**, 36 (1960).
11. K. W. Kleiner, F. E. Karasz, and W. J. MacKnight, *Polym. Eng. Sci.*, **19**, 519 (1979).
12. E. H. Kerner, *Proc. Phys. Soc.*, **69B**, 808 (1956).
13. J. C. Halpin and J. L. Kardos, *Polym. Eng. Sci.*, **16**, 344, (1976); also R. C. Progelhof and J. L. Thorne, *Polym. Eng. Sci.*, **19**, 493 (1979).
14. M. M. Dumoulin, P. J. Carreau, and L. A. Utracki, *Polym. Eng. Sci.*, **27**(20), 1627 (1987).
15. P. Sherman, *Industrial Rheology*, Academic, London, 1970.
16. R. Hill, *Mech. Phys. Solids.*, **11**, 357 (1963).
17. H. M. Smallwood, *J. Appl. Phys.*, **15**, 758 (1944).
18. T. Kunori and P. H. Geil, *J. Macromol. Sci. Phys.*, **B18**, 93 (1980).
19. Y. Sato and J. Furukawa, *Rubber Chem. Technol.*, **35**, 857 (1962).
20. R. A. Varin and D. Djokovic, *Polym. Eng. Sci.*, **28**(22), 1477 (1988).
21. L. E. Nielsen, *J. Appl. Polym. Sci.*, **10**, 97 (1966).
22. J. Leidner and R. T. Woodhams, *J. Appl. Polym. Sci.*, **18**, 1639 (1974).
23. J. Leidner and R. T. Woodhams, *J. Appl. Polym. Sci.*, **18**, 2637 (1974).
24. M. R. Piggott and J. Leidner, *J. Appl. Polym. Sci.*, **18**, 1619 (1974).
25. L. Nicolais and M. Narkis, *Polym. Eng. Sci.*, **11**, 194 (1971).
26. L. E. Nielsen, *J. Compos. Mater.*, **1**, 100 (1967).
27. T. Kunori and P. H. Geil, *J. Macromol. Sci. Phys.*, **B18**, 135 (1980).
28. M. Schragger, *J. Appl. Polym. Sci.*, **22**, 2379 (1978).
29. R. Greco et al., *J. Mater. Sci.*, **15**, 845 (1980).
30. G. P. Marshall, J. G. Williams, and C. E. Turner, *J. Mater. Sci.*, **8**, 949 (1973).
31. H. R. Brown, *J. Mater. Sci.*, **8**, 941 (1973).
32. J. G. Williams, *Fracture Mechanics of Polymers*, Wiley, London, 1984.
33. J. W. Teh, *J. Appl. Polym. Sci.*, **28**, 605 (1983).
34. A. G. Atkins and Y-W. Mai, *Elastic and Plastic Fracture*, Ellis Horwood/Wiley, Chichester, 1985.
35. C. B. Bucknall and M. M. Hall, *J. Mater. Sci.*, **6**, 95 (1971).
36. C. B. Bucknall, *Toughened Plastics*, Applied Science, London, 1977.

Received November 21, 1990

Accepted October 1, 1991